

BRIEF REPORTS AND COMMENTS

This section is intended for the publication of (1) brief reports which do not require the formal structure of regular journal articles, and (2) comments on items previously published in the journal.

High aspect ratio etching of atomic force microscope-patterned nitrided silicon

Steven A. Harfenist, Mehdi M. Yazdanpanah, and Robert W. Cohn^{a)}
*ElectroOptics Research Institute and Nanotechnology Center, University of Louisville,
Louisville, Kentucky 40292*

(Received 13 January 2003; accepted 3 March 2003; published 30 May 2003)

Silicon that is nitrided in a pure nitrogen plasma is patterned with voltage applied by an atomic force microscope (AFM). Wet chemical etching into AFM-patterned (110) silicon produced vertical trenches as narrow as 91 nm (for one 757 nm deep trench) and with aspect ratios as large as 8.9:1 (for a 95 nm by 849 nm trench). Compared to the ridge patterns resulting from AFM oxidation and wet etching of hydrogen-passivated silicon, a substantially higher applied voltage is required to pattern nitrided silicon. © 2003 American Vacuum Society. [DOI: 10.1116/1.1570848]

I. INTRODUCTION

Nanolithography using the atomic force microscope (AFM) is leading to less costly and simpler ways to prototype electronic, optical, and mechanical structures and devices. There have been numerous studies on anodic oxidation of silicon using the AFM.¹⁻⁴ High aspect ratio structures have been fabricated using the oxide as a resist to silicon etchants.⁵⁻⁷ When the goal is to fabricate isolated trenches, it would be desirable (in order to reduce writing time and AFM tip wear) to use a resist of opposite etch contrast to silicon dioxide, rather than writing the complementary oxide pattern over a much larger area. This objective of developing a contrast reversed process for AFM patterning of silicon motivated Sharma *et al.*⁸ to investigate the process of oxide patterning of silicon followed by nitridation of silicon in a pure nitrogen microwave-excited plasma. While the etch resistance of nitrided silicon to potassium hydroxide (KOH) proved to be many times greater than that of silicon dioxide, 2 to 3 nm high AFM-written oxide lines often did not develop into trenches on (100) silicon and never developed on (110) silicon. Based on x-ray photoelectron spectroscopy analyses that showed nitrogen penetration up to 6 nm into SiO₂, Sharma *et al.*⁸ concluded that the silicon underneath the thin AFM oxide had become nitrided, resulting in the loss of etch selectivity.

Herein, we report on a simple modification to Sharma's patterning process that does permit reverse contrast etching of AFM-patterned silicon. In the revised process, the silicon is first plasma nitrided, and then patterned by applying a voltage between the sample and the AFM tip. A raised pattern is produced that is similar in size and shape to the oxides fabricated by the standard anodic oxidation of hydrogen-

passivated silicon. KOH etches through the resulting pattern with adequate selectivity to produce deep vertical trenches.

The revised process is similar to Chien *et al.*'s studies where they blanket deposited a less than 5 nm thick layer of silicon nitride (by reacting SiCl₂H₂ with NH₃) on silicon, and then anodically oxidized the layer to produce silicon oxide. Removal of the oxide with HF and KOH transferred the oxide pattern into trenches in the silicon.⁹ The nitride resist layers of Chien⁹ and of Sharma⁸ are substantially different in growth process (as noted herein) and in composition. Chien's⁹ blanket deposition is pure Si₃N₄ while Sharma's⁸ nitrided silicon is a graded layer that contains only a fraction of silicon nitride (even at the surface) with some nitrogen present to a depth of 5 nm in (110) oriented silicon and 15 nm in (100) silicon.

II. TRENCH FABRICATION INTO PLASMA NITRIDED SILICON

Trenches are fabricated using the following procedure. Silicon is nitrided under conditions similar to those reported by Sharma *et al.*⁸ Specifically a *p*-type (110) silicon wafer, 1 to 10 Ω cm resistivity is cleaned in the following order: acetone, methanol, and isopropanol baths. It is immersed in a dilute hydrofluoric acid solution (200:1, H₂O:HF) for 60 s, rinsed in deionized water, and blown dry, leaving the silicon surface hydrogen passivated.¹ The silicon is nitrided in an ASTeX 5010 reactor chamber with an ASTeX 2115 microwave source. The reactor chamber is pumped only with pure nitrogen at 30 Torr pressure at 100 sccm. The silicon is exposed to the nitrogen plasma powered at 400 W with the microwave source for 1 h.¹⁰ Just prior to writing, the sample is rinsed in methanol and water and blown dry.

The nitrided silicon is patterned by scanning a voltage-biased AFM tip over the surface in tapping mode (intermit-

^{a)}Author to whom correspondence should be addressed; electronic mail: rwcohn@uofl.edu

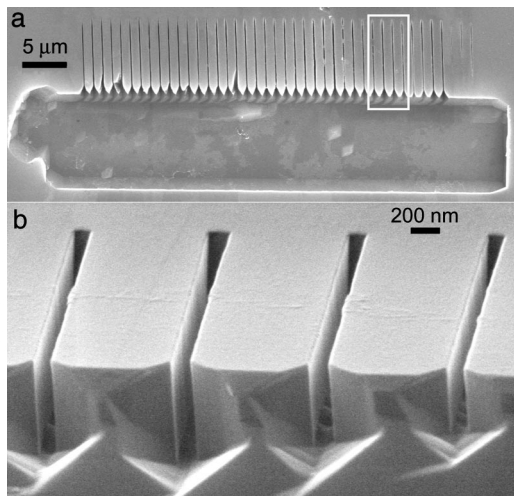


FIG. 1. Trenches produced by AFM patterning of nitrated (110) silicon followed by anisotropic etching. (a) Normal incidence SEM view of trenches fabricated by KOH etch followed by TMAH etch. (b) Grazing angle incident SEM image of the four trenches (written with 16 to 19 V) that are indicated by the white box in (a) [cf. Figs. 3(b) and 4 for trench dimensions].

tent contact) with a Thermomicroscopes Park M5 AFM. A focused ion beam-sharpened probe (Thermomicroscopes Ultralever FIB Cantilevers with a nominal cone angle of 5°) is used to reduce broadening of the tip during extended periods of writing. Before it is used, the AFM cantilever is sputter coated with ~ 5 nm of a Cr adhesion layer followed by ~ 20 nm Au to increase conductivity. A scanning electron microscopy (SEM) examination of tips metalized this way shows them to have radii of curvature from 20 to 30 nm. The cantilever has a resonance frequency of 320 kHz. The voltage applied to the tip is a 3 kHz square wave with zero dc offset. A number of lines are written in sequence at a tip speed of 200 nm/S with voltage increasing from ± 7.5 to ± 47 V. Following this, a 10 micron wide pattern is written transverse to the exposed lines for the purpose of producing a cross-sectional viewing trench in front of the desired trenches. The humidity is regulated between $35\% \pm 5\%$ during the exposure. Following voltage exposure, the sample is etched in 30 wt % KOH in water at 55°C for 9 min until the surface is seen to bubble (indicating a breakthrough into the underlying silicon) and followed up by etching at 75°C for 50 S in tetramethyl ammonium hydroxide (TMAH) (from Alfa Aesar premixed at 45 wt % in H_2O , which we then mixed 83 parts TMAH to 17 parts isopropanol).

Figure 1 shows the resulting trench patterns. The junction between the small trenches and the viewing trench shows faceting, which is typical of anisotropic wet chemical etching of silicon. The (111) plane vertical sidewalls in the trenches appear quite smooth, as do the sidewalls at the right-hand side of the large trench (sidewall image not shown). The AFM measured root-mean-square roughness of 2.1 nm at the bottom of the large trench appears in SEM images to be somewhat rougher than the trench sidewalls. At the far right-hand side of the parallel trenches are three incompletely etched trenches that were written from the right- to the left-

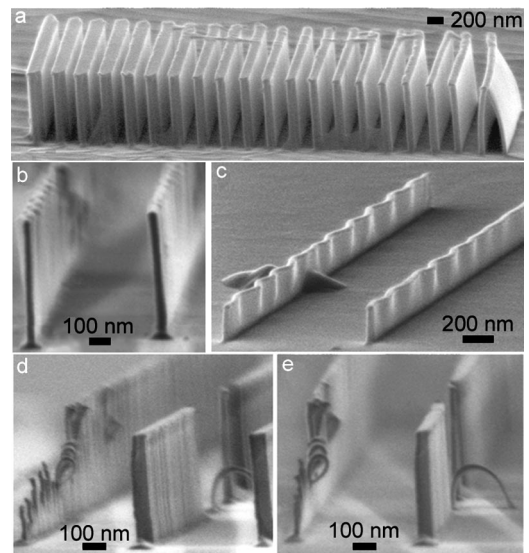


FIG. 2. Ridges produced by AFM patterning and TMAH etching of (110) silicon. (a) Grazing angle (80° sample tilt) SEM image of 830 nm high ridges ranging in width from 45 nm to 175 nm from the right- to the left-hand side. (b) Two ridges that show scalloping. (c) Two ridges that show scalloping that were intentionally written at 1° misalignment from $[-1, 1, -2]$ direction. (d) and (e) Two views of ridges that are partially dissolved resulting in a freestanding vertical nanorod and nanorods that have collapsed into arches.

hand side at voltages of ± 7.5 , 9, and 11 V. The lines to the left-hand side of the first three were written starting at ± 12 V and increasing to ± 47 V for the line on the extreme left-hand side. The patterns in this voltage range all developed into trenches after etching. Dimensional measurements of the written patterns and the etched trenches are reported in Sec. IV.

III. RIDGE FABRICATION ON HYDROGEN PASSIVATED SILICON

In order to better appreciate the lithography results on nitrated silicon, we also fabricated ridges by the existing process of anodic oxidation of hydrogen-passivated silicon,¹⁻⁴ followed by wet chemical etching in TMAH per the etch procedures in Refs. 5-7. This section reviews the fabrication process and presents the test structures that were fabricated. Then, Sec. IV compares the resulting dimensional measurements of the ridges against the trenches for various voltage exposure conditions.

(110) silicon is cleaned and hydrogen-passivated by the same procedure as described in Sec. II. Also, the AFM tip metalized similarly. The writing is done with a Thermomicroscopes contact Ultralever (force constant of 0.40 N/m and a probe tip cone angle of 25°) in contact mode at a set point force of 10.8 nN and a writing speed of 450 nm/s. Oxide lines are patterned on silicon using a 3 kHz square wave between ± 5 to ± 25 V. The silicon is etched in TMAH solution at 75°C for 75 S.

Figure 2(a) shows a series of 830 nm tall ridges, at a pitch of 285 nm, that result from the fabrication process. The narrowest ridge (written at the lowest voltage) is 45 nm wide

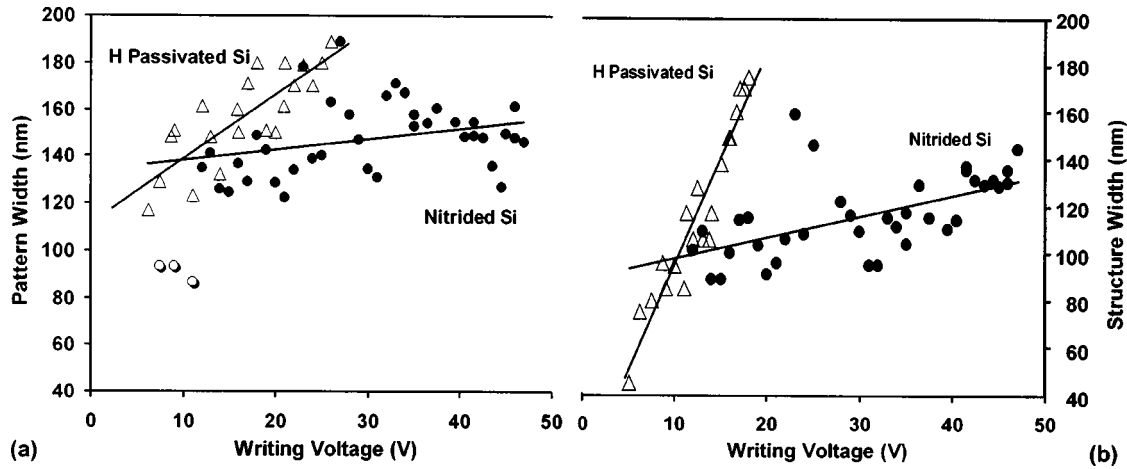


FIG. 3. (a) AFM pattern widths and (b) final etched structure widths for the structures in Figs. 1(a) and 2(a). Open circles represent AFM patterns that did not break through to form trenches.

and has collapsed into the neighboring ridge due to the capillary effect. This 18:1 aspect ratio structure is the highest aspect ratio structure we have made to date. It is certainly taller and has much smoother sidewalls than the 6:1 aspect ratio AFM patterned ridges produced by Chien *et al.*⁶ Their patterns were etched in KOH, which has a much lower silicon-to-oxide selectivity than does TMAH, and which tends to produce rough sidewalls.¹¹ Earlier work on AFM patterning of thin lines has been used to produce vertical ridges with aspect ratios of between 3:1 and 10:1 using anisotropic plasma etching of patterns written directly on silicon or on an organic resist layer over the silicon.^{12,13}

In addition to ridge collapse seen in Fig. 2(a), other limiting cases of etching are observed. Figure 2(b) shows two ridges of 35 and 45 nm width and each of 480 nm height which form a scalloped pattern with a period of 1 μm along the ridge. (The lines were written in contact mode with 2 kHz at ± 8 V and 300 nm/S tip velocity, followed by TMAH etching at 70 $^{\circ}\text{C}$ for 65 S.) The misalignment of the oxide patterns with respect to the silicon $[-1, 1, -2]$ direction may have caused the scalloping seen. Figure 2(c) shows a view of two other ridges each of 85 nm width and 255 nm high (written in tapping mode with 3 kHz at ± 8 V and 200 nm/S tip velocity) that exhibit scalloping along their lengths with a period of from 560 to 800 nm. The oxide patterns were purposefully written at a misalignment of 1 $^{\circ}$ with respect to the $[-1, 1, -2]$ direction while those aligned along the $[-1, 1, -2]$ [Fig. 2(a)] showed smooth sidewalls and no sign of scalloping. Figures 2(d) and 2(e) show (from two viewing orientations) nanowires that are formed by a combination of oxide dissolution and lateral sidewall etching. (Patterned in contact mode with a 2 kHz square wave at ± 7.5 V and 1 $\mu\text{m}/\text{S}$ writing speed, then etched in TMAH at 70 $^{\circ}\text{C}$ for 75 S.) The minimum width of the 450 nm tall ridges are 35 nm wide (left-hand side) and 55 nm wide (right-hand side) as measured from end-on SEM views. In Fig. 2(d), the vertical nanorod is more clearly seen, while in Fig. 2(e) the wire that has fallen over to form an arch is not obstructed in the view. Other curled wires that are not completely released from the

ridge are also evident on the ridge on the left-hand side. These results suggest that it is unlikely that the current process can be practically controlled to intentionally fabricate freestanding nanowires at specified locations. Nonetheless, these additional etching experiments are interesting in that they provide information on the limits of the AFM patterning and etching process.

IV. DIMENSIONAL COMPARISONS

Dimensional measurements of the voltage-induced patterns on the nitrided silicon and hydrogen passivated silicon were made using the AFM, while dimensions of the trenches and ridges in Figs. 1(a) and 2(a) were measured using a scanning electron microscope (LEO 1430) following sputter coating with 5–10 nm Au. The width of the voltage-induced patterns is reported as the full width at 10% maximum. The trench widths are measured from top view SEM images [e.g., the view in Fig. 1(a)] while the depth of the trenches are measured using near end-on views [e.g., Fig. 1(b)].¹⁴ The ridge widths are measured nearly end on at half-way between their top and bottom [e.g., Fig. 2(a)].

A. Dimensional data for hydrogen-passivated silicon

The dimensions of the oxide patterns and resulting etched ridges on hydrogen-passivated silicon are shown in Fig. 3. The data for the oxide and the ridges regress to straight lines with standard deviations of 11.6 nm and 11.7 nm and slopes of 2.7 and 9.0 nm/V, respectively. The narrowest oxide width of around 117 nm resulted in a 45 nm ridge, while the widest oxide of 189 nm resulted in a ridge of 175 nm width. These differences can be summarized by calculating the ridge thinning in a manner similar to calculating anisotropic etch selectivity. For the six highest voltages, the average thinning (per sidewall and with respect to measured oxide width) normalized by the 830 nm depth of etch is 149:1. However, for the six lowest voltages, the average thinning is 28:1. These large differences between the original oxide pattern width and etched ridge width are probably due to a combination of

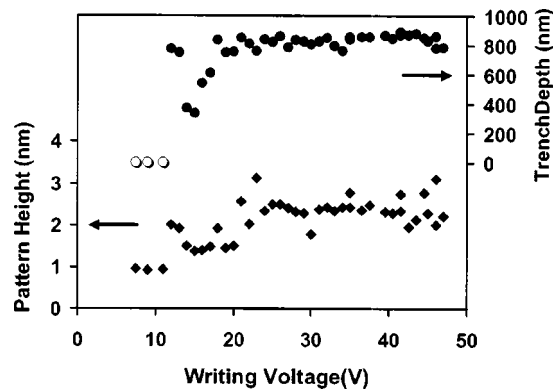


FIG. 4. Pattern heights and trench depths for the writing voltages for the trenches on nitrided silicon in Fig. 1(a). Open circles represent patterns that did not break through to form trenches.

two effects—a nonzero lateral etching rate in the $[111]$ direction, and thinner oxide at the edge of the oxide pattern (e.g., oxide patterns in Refs. 3 and 5 exhibit Gaussian-type shapes). For low voltages when the maximum oxide height is less than 3 nm (oxides ranged in height between 2.6 and 4.6 nm for all exposures), much of the oxide width at the edges is too thin to resist the etching solution. For higher voltages, the overall thicker oxide will have a greater percentage of its width able to resist the etchant, and then thinning is due mostly to the finite (111) to (110) selectivity of the TMAH solution.

B. Dimensional data for nitrided silicon

In Fig. 3, both pattern width and trench width regress to straight lines with a standard deviation of 13.9 nm and 26.3 nm, and slopes of 0.46 and 0.89 nm/V, respectively. These slopes, or sensitivity of width to patterning voltage, are much lower than for hydrogen-passivated silicon. The lower slope is due mostly to the electrically insulating nature of the nitrided layer. For most exposure voltages, the resulting trench widths are narrower than the pattern width. The slopes however indicate that the trench widths approach the pattern widths with increasing voltage. The reason for the trenches being narrower than the oxides is that the thin wings of the pattern do not sufficiently lower the etch resistance of the nitrided regions. However, as the voltage is increased, the patterns become thicker (at the 10% full width point) leading to wider trenches.

For voltage-patterned nitrided silicon, we obtain aspect ratios as large as 8.9:1 (for a writing voltage of ± 32 V) compared to 18:1 maximum for hydrogen-passivated silicon (reported in Sec. II). All depths and voltage-induced pattern heights for the nitrided silicon experiments are plotted in Fig. 4. Figure 4 shows that for 12 V and greater the pattern height increases to over 1 nm and the trenches develop. Between 14 to 17 V where the pattern heights are 1.4 to 1.5 nm, the trenches do not etch to their full depth. Yet for 19 and 20 V, the pattern height of 1.5 nm does lead to trenches of the full depth. This height appears to be somewhat marginal. All other oxides are between 1.8 to 3.1 nm and result in fully

developed trenches of depths between 748 and 890 nm. The differences in etch depth of 142 nm can be appreciated by considering differences in the time it takes to break through the AFM pattern. KOH etches (110) silicon at a rate of around 8 nm/S.¹⁵ A 142 nm variation corresponds to about an 18 S difference in breakthrough time. Continuing with this estimate TMAH (based on ridge etch rate of 830 nm/75 S) contributes 553 nm to etch depth and KOH contributes between 195 nm and 337 nm. (Note that when we only etched with KOH, we found the sidewalls to have extremely rough vertical striations, similar to the KOH etches reported in Chien *et al.*⁶)

Since the voltage-induced patterning of nitrided silicon is probably converting the silicon (and also possibly the nitride) into SiO_2 , it is worth comparing the KOH etch resistance of the pattern to that of pure SiO_2 . Our measured pattern breakthrough time of 9 min corresponds to a 4.5 nm SiO_2 resist thickness (using a published etch rate of 30 nm/h of SiO_2).¹⁵ For AFM oxidation of silicon, the total oxide thickness (oxide above and below the surface) is $1.75\times$ the oxide height⁴ and for AFM oxidation of thin layers of pure silicon nitride, the total oxide thickness is $1.85\times$ the height of the oxide pattern (for oxides of 2.33 nm height).⁹ Our pattern heights averaged 2.3 nm (for the trenches that fully developed) which using the values of subsurface oxide thickness from Refs. 4 and 9 predicts a total pattern thickness in the neighborhood of 4.0 to 4.3 nm. It is notable that the breakthrough time of SiO_2 and the pattern are comparable. Furthermore, given that the large viewing pattern completely developed, it appears that breakthrough occurs at the thickest portions of the pattern, not at the edge or an intermediate thickness of the profile of the pattern.

V. CONCLUSIONS

We have demonstrated that a light plasma nitridation treatment of silicon enables the contrast of AFM voltage patterning to be reversed with respect to hydrogen-passivated silicon. While higher voltage is required to produce patterns that develop under a combination of KOH and TMAH, the patterning of nitrided silicon, as compared to hydrogen-passivated silicon, requires much less patterning time when fabricating isolated trenches. While the largest trench aspect ratio of 8.9:1 is not as large as the 18:1 aspect ratio for ridges, this is to be expected given that lateral etching widens trenches and narrows ridges. Improved control of feature dimensions is anticipated by using carbon nanotube-tipped cantilevers (which are noted for greatly improved wear resistance and limited change in tip shape),^{16,17} and a controlled current source (which has been shown to improve dosage for thin insulating layers).¹³ Continued improvement of this and other AFM lithography processes points to affordable methods of prototyping three-dimensional nanostructures for applications in fundamental research and early product development.

ACKNOWLEDGMENTS

The authors thank Shashank Sharma for preparing the nitrogen-passivated silicon and Mark Crain for assistance in setting up the wet etching station. The study was supported by Army Research Office Grant Nos. DAAD19-01-1-0489 and DAAD19-00-1-0164, and National Aeronautics and Space Administration Cooperative Agreement NCC5-222.

- ¹J. A. Dagata, J. Schneir, H. H. Harary, C. J. Evans, M. T. Postek, and J. Bennet, *Appl. Phys. Lett.* **56**, 2001 (1990).
- ²J. A. Dagata, F. Perez-Murano, G. Abadal, K. Morimoto, T. Inoue, J. Itoh, and H. Yokoyama, *Appl. Phys. Lett.* **76**, 2710 (2000).
- ³J. A. Dagata, T. Inoue, J. Itoh, and H. Yokoyama, *Appl. Phys. Lett.* **73**, 271 (1998).
- ⁴F. Perez-Murano, K. Birkelund, K. Morimoto, and J. A. Dagata, *Appl. Phys. Lett.* **75**, 199 (1999).
- ⁵R. W. Cohn, S. F. Lyuksyutov, K. M. Walsh, and M. M. Crain, *Opt. Rev.* **6**, 345 (1999).
- ⁶F. S.-S. Chien, C.-L. Wu, Y.-C. Chou, T. T. Chen, S. Gwo, and W.-F. Hsieh, *Appl. Phys. Lett.* **75**, 2429 (1999).
- ⁷F. S.-S. Chien, E.-F. Hsieh, S. Gwo, A. E. Vladar, and J. A. Dagata, *J. Appl. Phys.* **91**, 10044 (2002).
- ⁸S. Sharma, M. K. Sunkara, M. M. Crain, S. F. Lyuksyutov, S. A. Harfenist, K. M. Walsh, and R. W. Cohn, *J. Vac. Sci. Technol. B* **5**, 1743 (2001).
- ⁹F. S.-S. Chien, J.-W. Chang, S.-W. Lin, Y.-C. Chou, T. T. Chen, S. Gwo, T.-S. Chao, and W.-F. Hsieh, *Appl. Phys. Lett.* **76**, 360 (2000).
- ¹⁰This nitridation condition was selected empirically from a variety of nitridation conditions as the one that produces the sharpest features by AFM patterning and etching. In S. Sharma *et al.*, *J. Vac. Sci. Technol. B* **5**, 1743 (2001) the exposure to nitrogen plasma was for 3 h at 550 W resulting in surface nitrogen concentration of 20% and penetration of nitrogen to a depth 5 nm. Thus, the sample reported on here would be expected to have even less surface nitrogen and a shallow penetration depth.
- ¹¹H. Seidel, L. Csepregi, A. Heuberger, and H. Baumgartel, *J. Electrochem. Soc.* **137**, 316 (1990).
- ¹²E. S. Snow, W. H. Juan, S. W. Pang, and P. M. Campbell, *Appl. Phys. Lett.* **66**, 1729 (1995).
- ¹³K. Wilder, C. F. Quate, B. Singh, and D. F. Kyser, *J. Vac. Sci. Technol. B* **16**, 3864 (1998).
- ¹⁴End-on SEM views were not used for trench width measurements due to potential viewing ambiguities caused by the facets.
- ¹⁵D. L. Kendall and R. A. Shoultz, *Handbook of Microlithography, Micromachining, and Microfabrication* (SPIE, Bellingham, WA, 1997), Vol. 2, Chap. 2, p. 74.
- ¹⁶H. Dai, J. H. Hafner, A. G. Rinzler, D. T. Colbert, and R. H. Smalley, *Nature (London)* **384**, 147 (1996).
- ¹⁷C. V. Nyguen, K.-J. Chao, R. M. D. Stevens, L. Delzeit, A. Cassell, J. Han, and M. Meyyappan, *Nanotechnology* **12**, 363 (2001).